

Determination of Thermal Conductivity of Some Shale Samples in Awi Formation and Its Geophysical Implications, Cross River State, Nigeria

A.J. Ilozobhie

Department of physics, University of Calabar, Nigeria

D. A. OBI

Department of Geology, University of Calabar, Nigeria

A.M. George

Department of physics, University of Calabar, Nigeria

O.A. Asuquo

Department of Physics, University of Calabar, Nigeria

Isah yahaya

Department of Physics, University of Calabar, Nigeria

Abstract

The thermal Conductivity of some about sixty – two (62) shale samples from four locations within the Awi formation using modified Lee's method were determined. It was observed that the thermal agitation in the sample increases as the temperature increases, after which thermal stability was attained. The Shale samples collected from location two and four tend to have high average thermal conductivity values ranging from 1.4490 W/m⁰C and 1.0802 W/m⁰C respectively while location one and three exhibits low values of thermal conductivity ranging from 0.8544 W/m⁰C and 0.7027 W/m⁰C respectively during the rising temperature measurement. During the falling temperature measurement location two and four still have high average thermal conductivity values of 1.3020 W/m⁰C and 0.9884 W/m⁰C respectively and location one has an average value of 0.8339 W/m⁰C while location Three has 0.6544 W/m⁰C. The low values exhibited by Location one and three is largely due to the fact that the outcrops in these locations were along the road and have been exposed to weather and human activities. However, the values from location two and four, suggests that shales within this location are post matured.

Keywords: Conductivity, agitation, stability, outcrops, post- matured

1. Introduction

Thermal conductivity (λ) is the intrinsic property of a material which relates its ability to conduct heat. Heat transfer occurs at a lower rate across materials of low thermal conductivity than across materials of high thermal conductivity. Correspondingly, materials of high thermal conductivity are widely used in heat sink applications and materials of low thermal conductivity are used as thermal insulation. The transfer of energy occurs as a result of collision among the particles of material involved, and the direction of heat flow occurs in the direction of decreasing temperature because higher temperature equates to high molecular energy or molecular movement thus, thermal conductivity increases with density.

Shale is a fine-grained sedimentary rock formed from the compaction of silt and clay size mineral particles that we normally called "mud". Correspondingly, most rock becomes more conductive with compaction as mineral to mineral contact increases. Shale typically show no such trend the reason being that their compaction involve repacking of phyllosilicates.

Published data on the thermal properties of shade are limited in number. Most of the identified studies show thermal conductivity of most shale of ambient conditions to be within the range of 0.5 to 2.2W/mK. Individual researchers have concluded that variables that affect thermal conductivity are dependent on the particular shale samples studied however factors such as composition, temperature, porosity, pressure and anisotropy are general factors that affects thermal conductivity of shale (Gillian and Morgan, 1987)

The study area is part of the Awi Formation of the Calabar flank of the Niger Delta in located Akamkpa Local Government Area of Cross River State. on the It is situated between latitude 5°15'N and 5°20'N and longitude 8°16'E and 8°21'E. (Fig 1.0a) The main access into this area is Calabar-Itu highway, which runs S-W direction. The study is aimed to determine the thermal conductivity of some shale samples within the Awi formation with a view to determine it's the geophysical implication(s) with respect to the formation area.

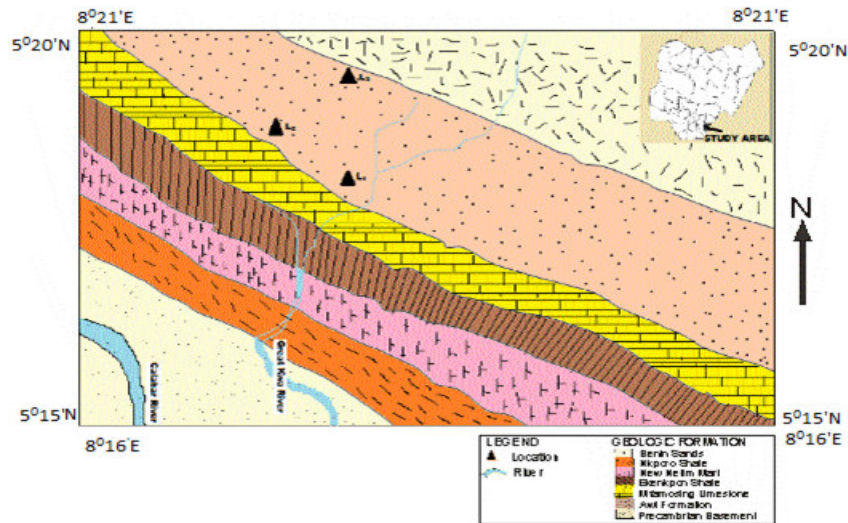


Fig. 1.0: Location of study area

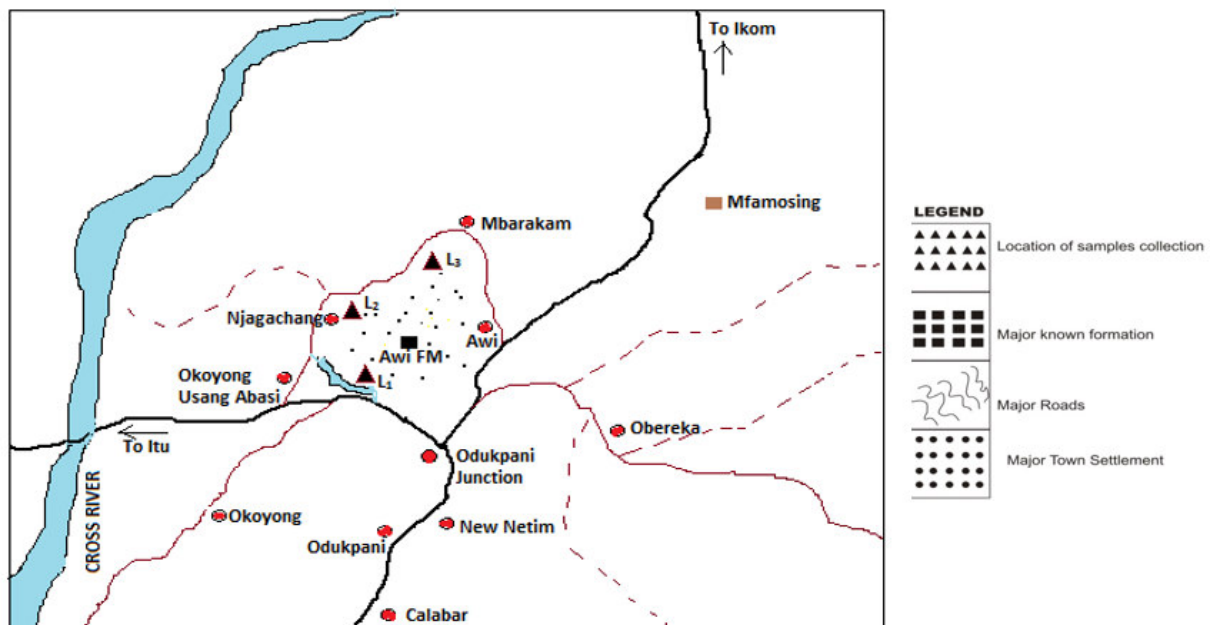


Fig. 1.0b: The study area with associated formations and towns

2. Geology of Study Area

The Calabar flank is part of the Southern Nigerian sedimentary basin that is bounded by the Oban-massif to the north and the Calabar Hinge line delineating the Niger Delta basin in the South (Nyong, 1995). It is also separated from the Ikpe platform to the west by a NE – SW trending fault (fig. 2.0). It served as the gateway of all marine transgression into the Benue Trough and is located between two hydrocarbon province, the Tertiary Niger Delta and the Cretaceous Douala Basin in Cameroun (Reijers and Peters, 1987).

The stratigraphic succession shows that the flank is mostly of Cretaceous-Tertiary age, comprising a basal Neocomian Aptian synrift fluvial sandstone, the Awi Formation and the marine post-rift of Odukpani group (Table 1.0). However, except for the basal fluvio-deltaic sands of Awi Formation, no evidence of deltaic sedimentation is present in the Calabar flank (Adeleye and Fayose, 1978).

Structurally, the Calabar Flank consists of basement horst and grabons (Fig. 2.0) that are aligned in a NE-SW direction like other South Atlantic marginal basins in West Africa (Reijers and Peters, 1987).

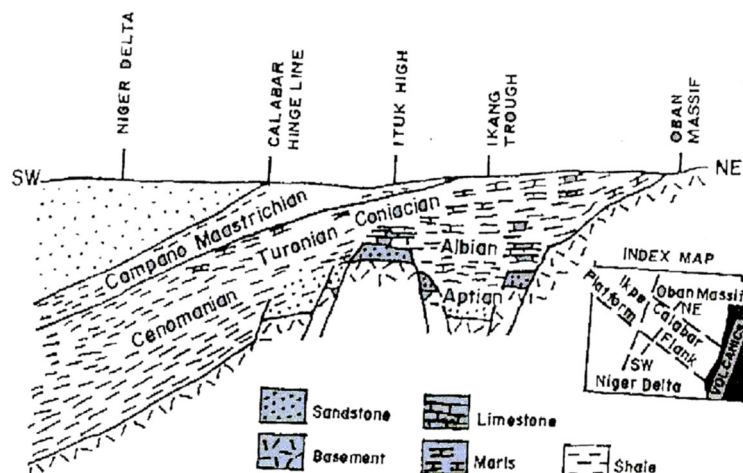


Fig.(2.0)::Structural Elements and Conceptual and subsurface distribution in Calabar Flank (After, Nyong, 1995)

Table 1.0: Stratigraphic sequence in the Calabar Flank

	AGE	FORMATION	LITHOSTRATIGRAPHIC	DEPOSITIONAL ENVIRONMENT
TERTIARY	Oligocene to recent	Benin formation	Pebbly sands and gravels	Continental
	Eocene	Ameke formation	Medium grained pebbly sandstones, clayey sandstones, calcareous silts, clay and thin limestones	Paralic
	Paleocene	Imo shale	Clayey shale, clay, ironstone bands, thin sandstone and sandy limestone bands	Paralic
CRETACEOUS	Maastrichtian	Nkporo shale	Gypsiferous dark grey shales with ironstone intercalation	Shallow marine
	Campanian		Unconformity	
	Santonian	New Netim	Marlstones with shale intercalations	Marine
	Coniacian	Marl		
	Turonian	Ekenkpon shales Nkalagu formation	Thick black pyritic shales with intercalations of mudstones, sandstones, ironstones and oyster beds	Marine
	Cenomanian			
	Albain	Mfamosing limestone	Stromatolitic fossiliferous limestones	Marine
	Aptian	Awi formation	Arkosic sandstones interbedded with shales	Fluvio-deltaic
Precambrian	Oban basement complex	Crystalline basement rocks		

3. Data Analysis

Geophysical work conducted by Odumodu (2012) to determine the temperature and geothermal gradient in the Calabar flank using the Bottom Hole Temperature (BHT) show the geothermal gradient in the area ranging from 30°C/Km to 45°C/Km increasing north - east with a corrected average of 38.8°C/Km. Chan et. al (2008) suggested that thermal and geothermal structures of a basin are essential data sets for the basin analysis concerning its hydrocarbon generation, retention and migration. Other geophysical works includes Barkers, (1996), Duncan and Mark (2000), Makhous and Galuchkin, (2005), Parker et. al (1961) Christopher, (2006).

Determination of Thermal Conductivity of Solids

There are various methods available for thermal conductivity measurement and each method depend mainly on configuration of a material. Some principal experimental methods are guarded heat flow, Surface Probe, Flash pulse system and the Lee's disc.

The Lee's Disc Method

This equipment consist of three brass disc A, B and C drilled to accept liquid-in-glass thermometer and a 6W electrical plate heater of the same diameter with the disc (Fig 3.0). It also consists of wooden stand with height of about 0.095m and with a separation of 0.075m between the wooden stands, with a total length of 0.010m, and a clamp to hold the disc together.

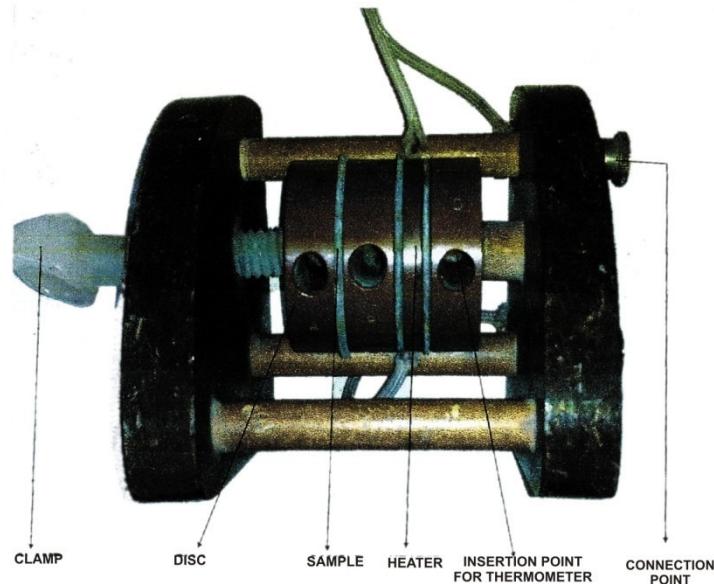


Fig. 3.0: The Lee disc equipment used for determination of thermal conductivities

This experimental method involves placing of the material whose conductivity is to be determined between specially designed discs. The method deals with the usage of electrical model, and a thermometer is used to detect the pulse heat response (Zmeskal et al 2003 and Griffin and George 2002). In this method heat moves from one disc to another. By measuring the difference in temperature of the disc, it is possible to determine the thermal conductivity of the material between the discs. This method is best for materials that are poor conductors. The value for the thermal conductivity (λ) of each sample of thickness d and radius r was estimated from the relation.

$$\lambda = \frac{ed}{2\pi r^2} \left[a_s \frac{T_A + T_B}{2} + 2a_A T_A \right]$$

Where, e is given by:

$$e = \frac{VI}{\left[a_A T_A + a_s \frac{T_A + T_B}{2} + a_B T_B + a_C T_C \right]}$$

and,

$$a_A = a_C = \pi r^2 + 2\pi r^2 l_d$$

$$a_B = 2\pi r^2 l_d$$

$$a_s = 2\pi r^2 l_s$$

Where,

l_d and l_s are the thickness of disc and sample, while a_A , a_B , a_C , and a_s are the exposed surface areas of the discs A, B, C and the specimen respectively. T_A , T_B and T_C are the temperatures of the discs A, B and C above ambient temperature. V is the potential difference across the heater and I is the current which flows through it. The materials used in this study include; Shale samples, Lee's Disc Apparatus, AC/DC power supply, An ammeter, A voltmeter, connection wires, a stop watch, cotton wool and four thermometers. A total of sixty four (64) shale samples were collected from four different locations within the Awi formation in Akamkpa and are kept in a black polythene bag in a cool place so that they are not expose to sun. Later, the samples were cut into slices of about 41mm in diameter and 2mm in thickness (Fig. 4.0). The surfaces of the samples were smoothed for good thermal contact. Each sample was placed between disc A and B one after the other. The heater was sandwiched between B and C, after tightening the clamp to hold all the discs together. The whole assembly was placed in an enclosure to minimize the effect of draught. A thermometer was placed close to the apparatus to measure the ambient

temperature Griffin and George (2002) and Duncan and Mark, (2000).

The schematic diagram for Lee's disc apparatus set up is shown in (fig 4.0),

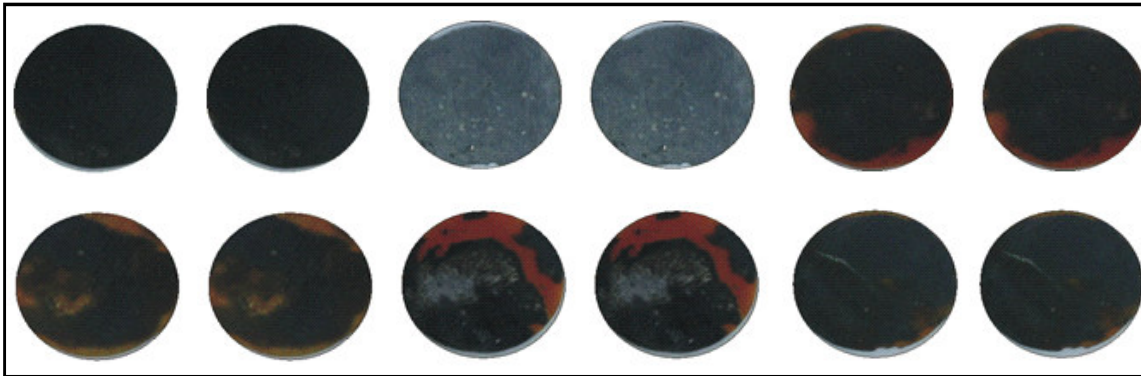


Fig. (4.0): Shale Samples at different Locations

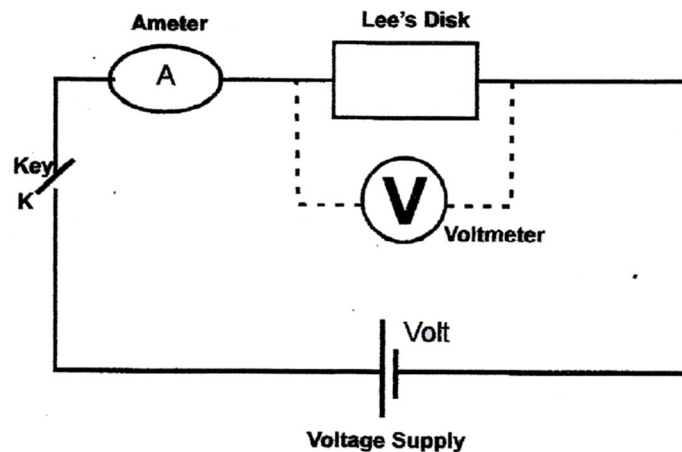


Fig. 5.0: Circuit diagram used for determination of the various thermal conductivities of shale samples

In order to effectively analyze thermal agitation of the sample, the thermal conductivity was estimated at every 10 minutes interval up to the point at which the temperatures of the discs has stabilized within $\pm 0.1^\circ\text{C}$ for at least 25 minutes.

4. Discussion of Results

A MATLAB programme was written to compute the thermal conductivities of the samples at a given interval. The results of the direct measurement of the samples at different current-voltage are shown in table 2.0 to 5.0 for both rising and falling temperature. The temperature of the shale discs increases up to stability for each disc. In addition, slight increase was noticed for ambient temperature. This could be attributed to increase in environmental activities at the vicinity of the experiment. The increase in temperature with time results to gradual decrease in thermal conductivity of the sample to equilibrium values.

Table 2.0: Variation of thermal conductivity of shale samples in location one

RISING TEMPERATURE FOR LOCATION ONE (1) CURRENT = 0.5A VOLTAGE = 9.6V							FALLING TEMPERATURE FOR LOCATION ONE (1)					
Time (min)	T _A (°C)	T _B (°C)	T _C (°C)	T _{AMB} (°C)	E (W/M ² .°C)	Λ (W/M.°C)	T _A (°C)	T _B (°C)	T _C (°C)	T _{AMB} (°C)	E (W/M ² .°C)	Λ (W/M.°C)
0	25	27	25	25	22.9344	1.2838	75	70	60	26	8.5655	1.4362
10	25	38	30	26	15.8178	1.5198	61	62	57	27	9.7765	1.3344
20	55	47	38	26	12.4976	1.5355	51	54	51	26	11.2937	1.2894
30	62	54	45	26	10.8679	1.5054	45	48	45	26	12.7779	1.2873
40	67	59	50	25	9.9416	1.4884	41	43	41	26	14.0787	1.2920
50	69	63	53	25	9.4854	1.4629	37	40	38	26	15.3351	1.2705
60	71	65	55	26	9.1867	1.4579	35	37	35	26	16.4625	1.2898
70	72	66	57	26	8.9904	1.4469	33	35	33	27	17.4472	1.2889
80	73	68	58	26	8.8247	1.4402	32	34	32	27	17.9850	1.2884
90	74	69	59	26	8.6932	1.4382	31	33	31	27	18.5571	1.2879
100	74	69	60	26	8.6434	1.4299	30	32	30	27	19.1668	1.2873
110	74	69	60	26	8.6434	1.4299	29	21	29	27	19.8980	1.2867
120	75	70	60	26	8.5655	1.4362	29	31	29	27	19.8180	1.2867
130	75	70	60	26	8.5655	1.4362						
140	75	70	60	26	8.5655	1.4362						
150	75	70	60	26	8.5655	1.4362						

Table 3.0: Variation of thermal conductivity of shale samples in location two

RISING TEMPERATURE FOR LOCATION TWO (2) CURRENT = 0.4A, VOLTAGE = 7.2V							FALLING TEMPERATURE FOR LOCATION TWO (2)					
Time (min)	T _A (°C)	T _B (°C)	T _C (°C)	T _{AMB} (°C)	E (W/M ² .°C)	Λ (W/M.°C)	T _A (°C)	T _B (°C)	T _C (°C)	T _{AMB} (°C)	E (W/M ² .°C)	Λ (W/M.°C)
0	29	29	29	29	12.0699	0.7831	68	62	58	30	5.5717	0.8468
10	41	35	32	30	9.6667	0.8853	57	56	55	30	6.2496	0.7968
20	49	42	38	30	8.0992	0.8865	49	50	50	30	7.0563	0.7737
30	55	47	43	30	7.2003	0.8846	44	45	45	30	7.8472	0.7726
40	58	51	47	30	6.7032	0.8687	39	40	40	30	8.8379	0.7713
50	61	54	50	30	6.3390	0.8641	36	37	37	30	9.5622	0.7704
60	63	57	52	30	6.0942	0.8581	35	36	36	30	9.8308	0.7700
70	64	58	53	40	5.9899	0.8568	28	29	29	30	12.2365	0.7668
80	65	59	55	30	5.8511	0.8500	28	28	29	30	12.5009	0.7831
90	66	60	56	30	5.7549	0.8479	31	33	31	27	18.5571	1.2879
100	67	61	57	30	5.6618	0.8479						
110	67	61	57	30	5.6618	0.8479						
120	68	62	57	30	5.6062	0.8521						
130	68	62	57	30	5.6062	0.8521						
140	68	62	58	30	5.5717	0.8468						
150	68	62	58	30	5.5717	0.8468						
160	68	62	58	30	6.5717	0.8468						

Table 4.0: Variation of thermal conductivity of shale samples in location three

RISING TEMPERATURE FOR LOCATION THREE (3) CURRENT = 0.35A, VOLTAGE = 6.9V							FALLING TEMPERATURE FOR LOCATION THREE (3)					
Time (min)	T _A (°C)	T _B (°C)	T _C (°C)	T _{AMB} (°C)	E (W/M ² .°C)	Λ (W/M.°C)	T _A (°C)	T _B (°C)	T _C (°C)	T _{AMB} (°C)	E (W/M ² .°C)	Λ (W/M.°C)
0	26	28	26	26	11.1024	0.6463	54	52	47	29	5.7714	0.6970
10	38	35	29	27	8.6672	0.7362	47	48	45	29	6.3196	0.6646
20	43	39	35	29	7.5196	0.7227	42	43	41	29	6.3196	0.6646
30	47	44	38	29	6.8474	0.7195	38	40	38	29	7.6362	0.6495
40	49	46	41	29	6.4863	0.7106	36	38	36	29	8.0554	0.6491
50	51	48	43	29	6.2117	0.7083	34	36	34	29	8.5232	0.6487
60	52	50	44	29	6.0556	0.7042	32	34	32	29	9.0487	0.6482
70	53	51	45	29	5.9332	0.7032	31	33	31	29	9.3366	0.6480
80	54	52	46	29	5.8156	0.7023	30	32	30	29	9.6433	0.6477
90	54	52	47	29	5.7714	0.6970	30	32	30	29	9.6433	0.6477
100	54	52	47	29	5.7714	0.6970	29	31	29	29	9.9709	0.6474
110	54	52	47	29	5.7714	0.6970	29	31	29	29	9.9709	0.6474
120	54	52	47	29	5.7714	0.6970	29	31	29	29	9.9709	0.6474
130	54	52	47	29	5.7714	0.6970						

Table 5.0: Variation of thermal conductivity of shale samples in location four

RISING TEMPERATURE FOR LOCATION FOUR (4) CURRENT = 0.4A, VOLTAGE = 9V							FALLING TEMPERATURE FOR LOCATION FOUR (4)					
Time (min)	T _A (°C)	T _B (°C)	T _C (°C)	T _{AMB} (°C)	E (W/M ² .°C)	λ (W/M.°C)	T _A (°C)	T _B (°C)	T _C (°C)	T _{AMB} (°C)	E (W/M ² .°C)	λ (W/M.°C)
0	30	30	30	30	14.5844	0.9789	80	72	64	30	6.0713	1.0855
10	44	38	33	30	11.3834	1.1190	55	54	53	30	8.1012	0.9966
20	51	47	41	30	9.4582	1.0783	48	48	47	30	9.1893	0.9868
30	63	54	47	30	7.9773	1.1227	43	43	43	30	10.1752	0.9789
40	67	58	51	30	7.4351	1.1129	41	41	41	30	10.6715	0.9789
50	69	61	54	30	7.1199	1.0978	39	39	39	30	11.2188	0.9789
60	71	63	57	30	6.8537	1.0874	38	38	38	30	11.5140	0.9789
70	72	64	58	30	6.7480	1.0857	36	36	36	30	12.1537	0.9789
80	73	66	59	30	6.6235	1.0806	35	35	35	30	2.5009	0.9789
90	75	67	60	30	6.4865	1.0872	34	34	34	30	12.8686	0.9789
100	76	68	61	30	6.3918	1.0856	33	33	33	30	13.2586	0.9789
110	77	69	62	30	6.2998	1.0841	33	32	33	30	13.3469	0.9851
120	80	71	63	30	6.1227	1.0945	32	32	32	30	13.7669	0.9853
130	80	72	64	30	6.0713	1.0855	32	31	32	30	13.7669	0.9853
140	80	72	64	30	6.0713	1.0855	31	31	31	30	14.1140	0.9789
150	80	72	64	30	6.0713	1.0855	31	31	31	30	14.1140	0.9789

Figure 4.0 to 11.0 shows the variation of the thermal conductivities with time for the four location samples. The thermal agitations of the samples were found to increase gradually and approaches stability with time. The samples attained equilibrium after 120minutes for rising temperature of continuous agitation. The rate at which thermal equilibrium was attained was found to be faster at the falling temperature than rising temperature. This effect could be attributed to the fact that initially, enough energy is required to break the bonds of the particles in the samples and on reaching their maximum excited positions, as the thermal energy reduces, the particles tend to return back to their mean position faster and more regular than when the temperature was rising.

It is evidence that as the temperature of the samples increases, the particles receive thermal agitation and thereafter scatter away from their equilibrium position. This is more prominent at the rising temperature. Therefore, the values of the thermal conductivities obtained confirm that the samples possess good thermal behavior. However, the shale samples from location1 with an average thermal conductivity of about have higher thermal agitation and conductivities than the shales from other locations.

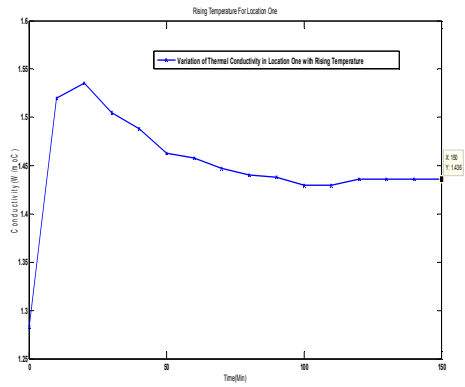


Fig. : 6.0: Variation of thermal conductivity in location one with rising temperature

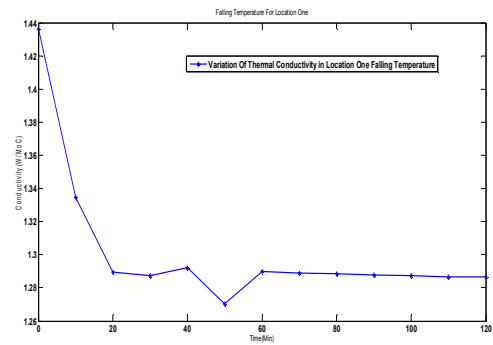


Fig. : 7.0: Variation of thermal conductivity in location One with falling temperature

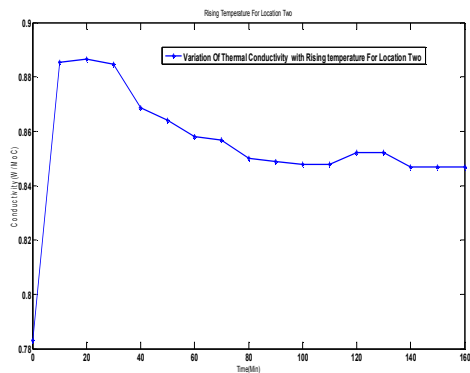


Fig. : 8.0: Variation of thermal conductivity in location Two with rising temperature

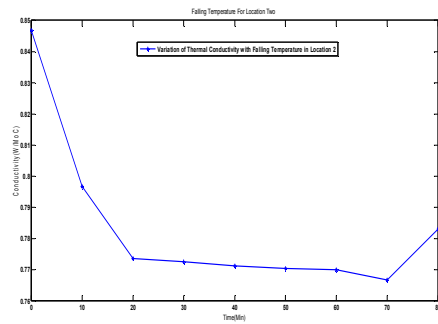


Fig. : 9.0: Variation of thermal conductivity in location Two with falling temperature

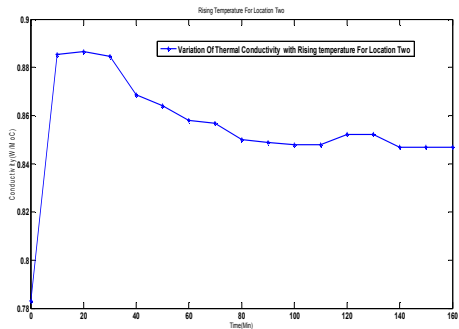


Fig. : 8.0: Variation of thermal conductivity in location Two with rising temperature

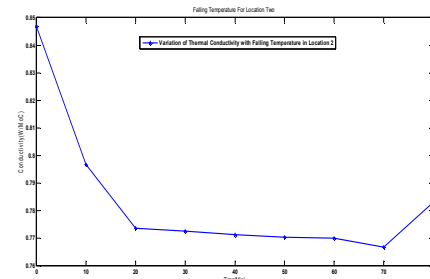


Fig. : 9.0: Variation of thermal conductivity in location Two with falling temperature

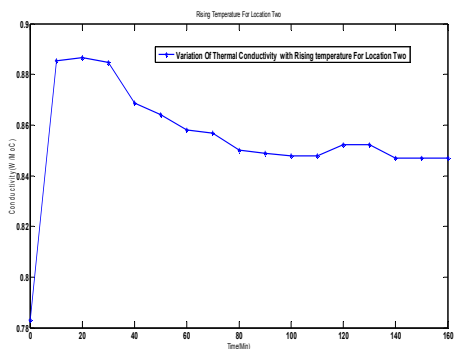


Fig. : 8.0: Variation of thermal conductivity in location Two with rising temperature

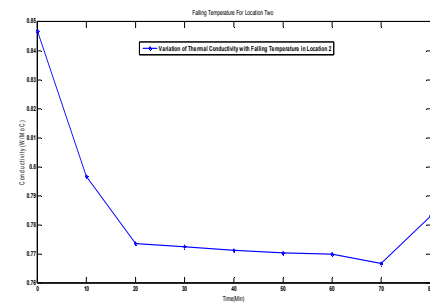


Fig. : 9.0: Variation of thermal conductivity in location Two with falling temperature

Geophysical implications

The plots (fig.6.0 to fig.13.0) of measured thermal conductivity (λ) with time shows that the shale samples from location 1 to 4 exhibit linear increase in thermal conductivity with time 10minutes – 20minutes followed by drastic fall in thermal conductivity followed with fluctuating variation of (λ) and a steady value of (λ).

Figs. (6.0, 8.0, 10.0 and 12.0) depicts the variation of the thermal conductivities with increase in temperature of the shale samples from the different locations within the study area. The normal increase in thermal conductivity values with increase in temperature for shale was shown by the plots. The conductivity of these shale samples tends to have high falling value within time range from 0-30 minutes however shales from location one and three shows a sharp drop in thermal conductivity values from their various peak values and this is followed by fairly steady values with temperature. Location two maintain stable values of thermal conductivity with time from its peak value before steady falling in values while location four shows erratic fall and rise.

Figs. (7.0, 9.0, 11.0 and 13.0) depicts the variation of the thermal conductivities with falling in temperature of the shale samples from the different locations within the study area. All the plots show a gradual decrease with temperature with time.

The shale samples from Location one and three shows erratic thermal conductivity distribution which may be as a result of exposure of the samples to weather and human activities which may weaken the conductivity properties of the shales, while the other region of thermal stability indicate uniformity in shale composite and texture.

The region of linear relationship with falling in temperature in locations (2) and (4) may indicate that the shales have excellent thermal conductivity properties that allowed maturation and migration of hydrocarbon to be effective. The burial and temperature history for this formation demonstrate that the shale may have entered the oil window approximately 60Ma and were exposed to temperatures as high as 125°C probably over a period of 50 years before uplift.

5. Conclusion

The study examined the thermal conductivity of some shale samples in Awi formation with time interval of 10minutes to 160minutes. The average thermal conductivity for the various locations ranged from 0.6463 ($\text{Wm}^{-1}/^{\circ}\text{K}$) to 1.5355 ($\text{Wm}^{-1}/^{\circ}\text{K}$). Therefore, thermal conductivity of shale in the formation exhibits a northeastern directional trend increase. The burial and temperature history for this formation demonstrate that the shale may have entered the oil window approximately 60Ma and were exposed to temperatures as high as 125°C probably over a period of 50 years before uplift.

Therefore, this study on thermal conductivity on shales within Awi formation in line with Geothermal studies in Calabar flank (Odumudo, 2010), shows that thermal conductivity can be used in determining the maturation of shale and as such the shales in this area are post-matured because they are highly influenced by the temperature regime in the area..

REFERENCES

- Adeleye, D. R. and Fayose, E. A. (1978): Stratigraphy of the type section of Awi formation, Odukpiani Area Southern Nigeria. *Journal Min. and Geology* Vol. 15 (1) pp. 33-37.
- Barker, C. (1996). *Thermal Modeling of Petroleum Generation: Theory and Applications in Developments in Petroleum Geosciences*: Amsterdam, Elsevier, V. 45, pp. 512.
- Christopher, D. Laughrey (2006). Thermal maturity of Devonian Black Shale-gas reservoirs, Northwestern Pennsylvania evidence from Organic Petrology Geochemistry, and Mineralogy. *Pennsylvania Geological Survey*: pp. 53.
- Duncan, M. P., and Mark, J. (2000). Thermal Conductivity of PTFE and PTFE Composites IPTME, Loughborough University, Loughborough, UK. Pp. 580 – 581.
- Gillian, T.M and I. L. Morgan (1987): *Shale: Measurement of thermal properties*. Oak Ridge Laboratory, USA. pp 1-10.
- Griffin and George (2002). Lee's Conductivity Apparatus (Electrical Method) LL44 – 590 1.3. 1122/7303, Griffin and George Ltd. Wembley, Middlesex UK. Pp. 2 – 4.
- Makhous, M. and Galuchkin, Y. (2005). Temperature and Geothermal Gradient Fields in the Calabar Flank and Parts of the Niger Delta, *Petroleum Technology Development*, Vol. 2; (No 2) pp 1 -15.
- Nyong, E. E. (1995). *Cretaceous Sediments in the Calabar Flank: A Geological Excursion Guide Book to Oban Massif, Calabar Flank and Manfe Embayment, Southeastern Nigeria*. Ford Publishers: Calabar, Nigeria.
- Odumodu, C. F. (2012). Temperatures and Geothermal Gradient Fields in the Calabar Flank and parts of the Niger Delta, Nigeria. *Journal of Petroleum Technology Development*, Vol 2 (No 2) pp 1-15.
- Parker, W. J., Jenkins, J. J., Butler, C. P. and Abbott, G. L. (1961). A Flash Method of Determining Thermal Diffusivity, Heat Capacity and Thermal Conductivity, *Journal of Applied Physics*, 32(9), 1679 – 1684..
- Reijers, T. J. A. and Petters, S. W. (1987). Depositional Environment and Diagenesis of Albian Carbonates in

Calabar Flank, S. E. Nigeria. *Journal of Petroleum Geology* (10), 283 – 299.
Zmeskal et al (2003). Thermal Conductivity in Centinuuous Metal Matrix Composites with Random Distributions, *Material Science Forum*, Vols 426 – 432, 2169 – 2174.